

Impact of discharge voltage on wall-losses in a Hall thruster

S. Mazouffre, K. Dannenmayer, and C. Blank

ICARE, CNRS, 1C avenue de la Recherche Scientifique, 45071 Orléans, France

(Received 21 March 2011; accepted 24 April 2011; published online 6 June 2011)

Calibrated infrared thermal imaging is used to investigate the temperature of the BN-SiO₂ discharge chamber walls of the high-power PPSX000-ML Hall thruster over a broad voltage range. The energy flux deposited by charged particles onto the channel walls is assessed by means of a semi-empirical time-dependent thermal model. Equilibrium temperature as well as power losses onto the channel walls are determined for low and high voltage operation states. For a given input power, the two quantities strongly depend upon the discharge voltage. Above ~ 500 V, losses augment in an exponential way whereas they vary linearly at low voltages. As suggested by many theoretical works, secondary electron emission yield and associated near-wall sheath potential lowering could explain experimental outcomes. The contribution of ion bombardment, however, cannot be fully ruled out, as shown here. © 2011 American Institute of Physics. [doi:10.1063/1.3592251]

A Hall thruster is a discharge in a crossed electric and magnetic field configuration for spacecraft propulsion purposes.^{1,2} A low-pressure xenon discharge is confined within an annular chamber with dielectric walls. A set of coils provides a radially directed magnetic field with a maximum strength at the channel exhaust. The magnetic field is chosen strong enough to trap electrons, but weak enough not to affect ion trajectories. The potential drop is mostly concentrated in the final section of the channel owing to the low electron transverse mobility in this area. The corresponding axial electric field accelerates ions out of the channel, which generates thrust. Hall thrusters are currently employed for geosynchronous satellite orbit correction and station keeping. Such a propulsion technology is also well adapted for satellite orbit transfer maneuvers and interplanetary journeys of robotic space probes.

The thermal state of a Hall effect thruster, which originates in the interaction between the plasma and the discharge chamber walls, has a drastic impact upon the operation envelope, the performance level, and the thruster lifetime. The acquisition of reliable data about temperature of thruster elements and energy loss mechanisms are therefore of great relevance for existing thruster optimization and for the development of low and high power devices. The thermal behavior of channel walls was recently investigated for several Hall thrusters by means of calibrated thermal imaging.^{3,4} In addition to the steady-state temperature, the energy flux transferred to the walls by the plasma was inferred from measurements in transient regime combined with a time-dependent thermal model of the thruster. Those studies were focused on the influence of the operating parameters as well as the channel dimensions and material upon the thermal load and energy losses. It was for instance shown that losses decrease with the size and are the lowest when BN-SiO₂ is used. Nonetheless, most of the measurements were at that time limited to the low voltage range, i.e., below 500 V. In this contribution, the thermal state of the PPSX000-ML Hall thruster BN-SiO₂ channel

walls is interrogated by way of infrared imaging over a broad voltage range, namely from 300 up to 1000 V.

Hall thruster infrared image acquisition was accomplished with a calibrated infrared camera suited for the 8–9 μm spectral domain.³ The camera covers a temperature range from -20 to 1500°C with a frame rate up to 750 Hz. Experiments were conducted in the PIVOINE test bench with the infrared camera located 180 cm from the thruster exit plane. The observation angle was 50° , in which case the camera viewed virtually the entire thruster. Observation was carried out through a CaF₂ window. In order to enable absolute temperature determination for the thruster channel walls, the normal spectral emissivity of the BN-SiO₂ material was measured in air as a function of temperature.³ Within the 8–9 μm spectral band the emissivity does not change much with temperature. The mean emissivity is 0.92.

In Fig. 1, the equilibrium channel wall temperature T_{wall} is plotted as a function of the electrical input power $U_d \times I_d$ for the PPSX000-ML thruster fired with a fixed coil current. The wall temperature is defined as $T_{\text{wall}} = \frac{1}{2}(T_{\text{ext}} + T_{\text{int}})$, where T_{ext} is the mean external wall temperature and T_{int} is the mean internal wall temperature. Temperatures are measured in steady state in the final section of the channel where most of the energy is lost.

At low voltage, $U_d < 500$ V, T_{wall} varies smoothly over a broad range of applied power. The T_{wall} values follow the same distribution law whatever the (U_d, I_d) pair. As shown in a preceding study,³ the relation between T_{wall} and P can be written in the form

$$T_{\text{wall}} = 270 + bP^n. \quad (1)$$

Coefficients b and n characterize somehow power losses and thruster efficiency.³ The parameter b depends on the wall material and the geometry. The exponent n is solely connected with the material. One finds: $b = (23 \pm 5) \text{ KW}^{-n}$ and $n = (0.38 \pm 0.02)$. These values are in agreement with

the ones obtained with other thrusters equipped with BN-SiO₂ walls.³

At high voltage, $U_d \geq 500$ V, the evolution of the wall temperature with the input power seemingly departs from the aforementioned power law as illustrated in Fig. 1. For a given power level, T_{wall} rises quickly with the voltage when the latter is above ~ 500 V. It is well known that the properties of a Hall thruster discharge, e.g., the current oscillation amplitude and frequency, change with the applied voltage in a complex way.⁵ In any case, the observed drastic increase of T_{wall} with the applied voltage means the energy flux delivered by the plasma to the wall raises. Therefore the discharge characteristics must change either in the bulk or within the sheath. One way to get insight into the mechanism at work is to quantify the energy flux. This can be achieved by means of temperature measurements in transient regime.

A time-dependent thermal model of a Hall effect thruster channel relies on the energy conservation equation and a set of simplifying assumptions.⁴ Instead of performing a full calculation of energy transfers, an option consists in treating the problem of radiation exchange in a thermal enclosure. The latter is defined by the channel walls, and the impact of other thruster components are simulated by an isothermal surface surrounding the channel.⁴ Our physical model then reduces to the well-known unsteady heat-conduction equation with no sources or sinks⁴

$$\frac{\partial T(r, t)}{\partial t} = \alpha \frac{\partial^2 T(r, t)}{\partial r^2}, \quad (2)$$

where α is the thermal diffusivity. The energy rates are: a conductive heat flux through the channel walls, a radiative flux for all surfaces ϕ_{rad} , the energy deposited by the plasma q_p , which is an unknown variable and for the outer side of the external dielectric wall, a thermal radiation heat flux towards the outside ϕ_{outside} . The appropriate boundary conditions therefore read:

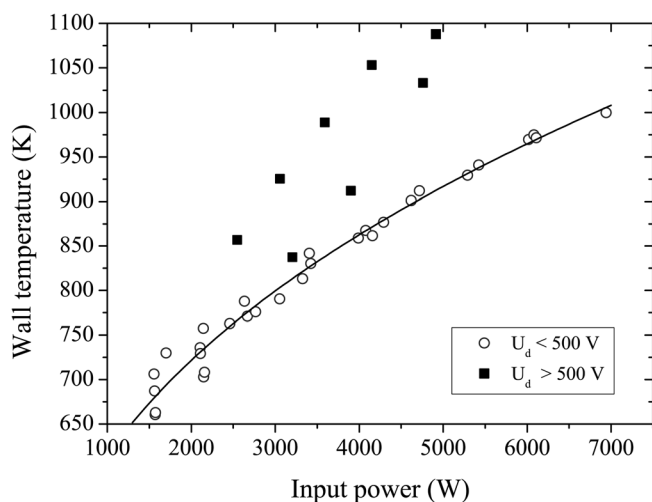


FIG. 1. Equilibrium wall temperature against input power. Datapoints are split into two groups: $U_d < 500$ V and $U_d > 500$ V. The line corresponds to a curve fitting with the power law $T_{\text{wall}} \propto P^{0.38}$.

$$\kappa \left. \frac{\partial T}{\partial r} \right|_{r=0} = -\phi_{\text{rad}} + q_p, \quad (3)$$

for both the internal and the external walls,

$$\begin{aligned} \kappa \left. \frac{\partial T}{\partial r} \right|_{r=h} &= -\phi_{\text{outside}} \quad \text{for the external wall} \\ &= 0 \quad \text{for the internal wall,} \end{aligned} \quad (4)$$

where κ is the thermal conductivity and h is the wall thickness. The thermal enclosure is composed of 5 surfaces that are individually isothermal. Radiative fluxes are then computed by means of grey body configuration factors G .⁶ To compute the temperature of a given channel section implies to know at each time step the temperature of all other parts as well as the distribution of the energy flux q_p . Here, numerical simulations use, as input data, measured temperature fields. Advantages of this semi-empirical approach are twofold, namely: it allows to drastically reduce the number of parameters and it brings closer the simulations to the real thermal behavior of the thruster.

The unknown quantity q_p is obtained by adjusting in an iterative manner the calculated temperature profile to the one measured by means of calibrated infrared imaging. Contrary to our preceding study,⁴ differential equations are solved in two steps by a Runge-Kutta 2 algorithm using the Heun predictor-corrector method. Furthermore, an optimization algorithm was added. Note that new values of G factors are also used in this work. In the range of electrical power of interest, i.e., 1–7 kW, typical values for q_p lie in the range 0.1–5 W/cm².

In Fig. 2, q_p is plotted as a function of the applied voltage for the inner and outer wall of the PPSX000-ML thruster. The flux q_p depends strongly, and in a non-linear way, upon the applied voltage U_d . The quantity q_p also increases with the injected xenon mass flow rate due to an increase in the amount of ions produced inside the channel. Another way to

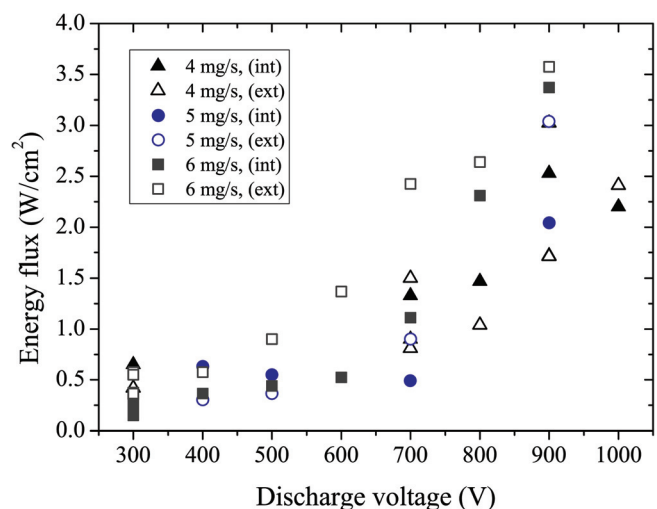


FIG. 2. (Color online) Power per unit area q_p delivered by the plasma onto the channel dielectric walls against the discharge voltage: internal wall (full symbol) and external wall (open symbol). The xenon mass flow rate is varied from 4 to 6 mg/s.

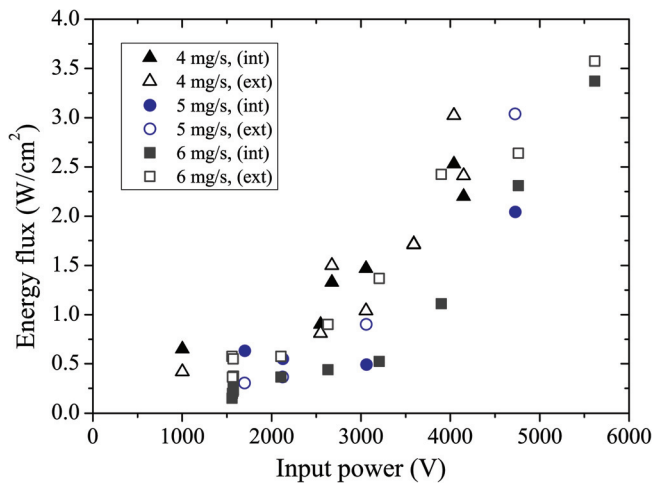


FIG. 3. (Color online) Power per unit area q_p delivered by the plasma onto the channel dielectric walls as a function of the input electrical power for three values of the mass flow rate: internal wall (full symbol) and external wall (open symbol).

present obtained data is to plot q_p as a function of the input electrical power. The resulting graph is shown in Fig. 3. The trend is naturally similar to the one depicted in Fig. 2. The amount of power delivered to the dielectric wall increases with the input power. The graph also shows that for a fixed input power, seeded mass flow rate, and applied voltage do not have the same impact on q_p . Power losses are mainly driven by applied voltage. In Figs. 2 and 3 the evolution of q_p changes suddenly when U_d is above ~ 500 V, as does the equilibrium temperature.

In Fig. 4, the amount of power passed to the BN-SiO₂ walls P_{wall} is plotted as a function of the input electrical power. At low voltage, i.e., $U_d < 500$ V, P_{wall} is a small fraction of the applied power. Besides, it varies linearly with the applied power. At high discharge voltage, i.e., $U_d \geq 500$ V, departure from the linear evolution occurs as exemplified in Fig. 4. The fast increase of T_{wall} above 500 V, see Fig. 1, therefore, originates from the rapid growth of energy losses. P_{wall} reaches up to 20% of the applied power when the

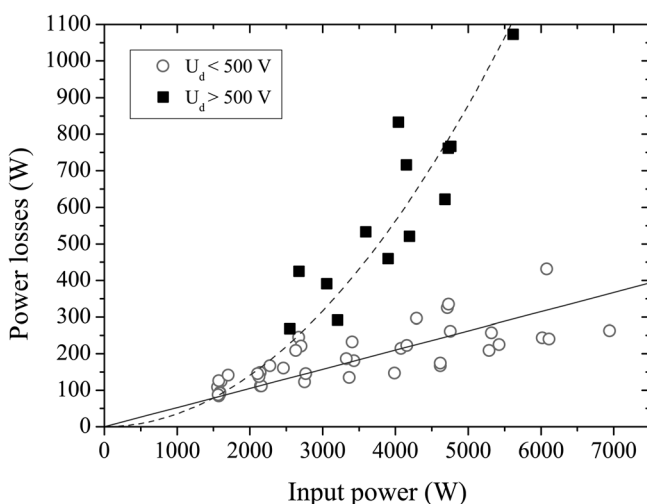


FIG. 4. Power losses on walls against input electrical power. Data is divided into two groups: $U_d < 500$ V and $U_d > 500$ V. Solid line is a linear fit. The dashed line is a power law fit ($P^{1.6}$) through the high voltage range.

PPSX000-ML thruster is operated at 1000 V. Above 500 V, datapoints can seemingly be fitted to a power function: $P_{\text{wall}} \propto P^{1.6}$. The evolution of the two quantities T_{wall} and P_{wall} with the input power is quite complicated as two regimes must be distinguished according to the voltage. A possible interpretation involves plasma sheath dynamics, as we shall see in the remainder of this paper.

Production of multiply charged ion species in the discharge core is of course a means for increasing losses to the walls as ion kinetic energy depends on the electrical charge. However, it cannot justify alone the measured trend since the fraction of multiply charged ions augments linearly with U_d .⁷

A first-order approximation, i.e., a picture with only Xe⁺ ions, in which the electron contribution is neglected and plasma sheath properties are fixed, indicates the amount of power transferred to the channel walls depends upon both the ion kinetic energy and the ion current to the walls.³ Assuming the electric field distribution does not change with thruster parameters, the former is proportional to the discharge voltage. The latter can be expressed as a fraction of the discharge current. Hence, one would expect P_{wall} to vary as $U_d \times I_d$. This is obviously not the case at high discharge voltage, which indicates an additional mechanism must be put forward.

In preceding works, the axial velocity component of Xe⁺ ions was measured by means of laser-induced fluorescence spectroscopy at 834.72 nm along the channel centerline of the PPSX000-ML Hall thruster for several operating conditions.⁸ In Fig. 5, the Xe⁺ ion kinetic energy in axial direction $E_{k,x}$ is plotted as a function of the input power. The kinetic energy is here given at the channel outlet. It therefore corresponds to the potential drop experienced by ions before leaving the channel. It also provides information about the fraction of accelerating electric field inside the channel.⁸ One dataset was constructed at 300 V varying the anode mass flow rate. The other dataset was obtained at 6 mg/s by changing U_d up to 700 V. To a large extent, curves in Fig. 5 resemble curves in Fig. 4. At low voltage, the ion kinetic

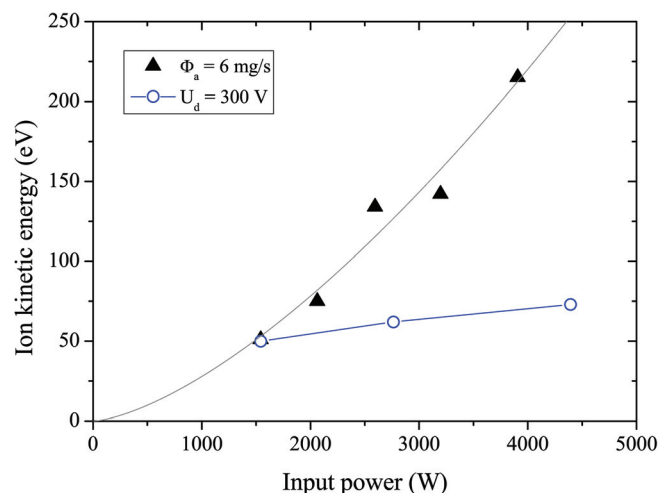


FIG. 5. (Color online) Xe⁺ ion axial kinetic energy at the channel exhaust against applied power: mass flow rate series at 300 V (circle), voltage series at 6 mg/s (triangle). The line is a power function fit ($P^{1.5}$) to voltage series points.

energy varies linearly with P . At high voltage, the kinetic energy grows in an exponential way: $E_{k,x} \propto P^{1.5}$. The exponential value is close to the one found for P_{wall} , see Fig. 4.

At first sight, our set of results suggests the energy flux deposited by the plasma onto the thruster channel walls is mostly determined by the ion kinetic energy. The observed high-voltage trend for T_{wall} and P_{wall} would then be a consequence of the rapid increase of the ion kinetic energy with U_d . However, the relationship between the ion axial kinetic energy and P_{wall} must be treated with caution. Indeed, to date, there is no direct evidence that the component of the ion velocity directed towards the dielectric walls varies in a non-linear way with U_d . At this stage, results rather indicate the change in electric field distribution as well as the change in power losses at walls could be driven by the same physical mechanism.

A credible explanation for the impact of discharge voltage on P_{wall} and $E_{k,x}$ is linked to the near-wall plasma sheath properties. At high voltage, i.e., at high electron and ion energy, the secondary electron emission (SEE) from the wall can be so large that it compensates for the incoming electron flux. In that case, the sheath strength diminishes abruptly due to space charge saturation, which means the potential drop that usually repels electrons vanishes.⁵ The consequence is a large particle flux to the dielectric wall, hence a large energy transfer.^{9,10} Reduction of the plasma sheath potential at high voltage certainly modifies the near-wall electron conductivity. Besides, the release of cold electrons by the walls, in comparison with bulk electrons, changes the plasma properties, which as a related effect changes the electron mobility across the magnetic field in the plasma core. Variation of both electron mobility contributions certainly leads to a noticeable distortion of the electric field distribution with the voltage which could translate into a fast increase of the ion axial kinetic energy inside the channel.

The threshold value between the low-voltage and the high-voltage cases lies between 400 and 500 V according to our measurements. The threshold is surely connected with the SEE yield of the wall material. It is likely to depend on

the propellant gas which influences plasma properties. Moreover, it might depend on the channel geometry that specifies to a large extent the charged-particle flux per unit area.

The contribution of the present study is threefold. First, it illustrates experimentally the non-linear evolution of the energy flux to the Hall thruster walls at high discharge voltages. Second, it reveals an apparent link between power losses at walls and ion axial kinetic energy inside the channel. Third, it makes an attempt to explain the temperature, power losses, and ion velocity measurements, which involves secondary electron emission by walls. Further investigation, e.g., with various wall materials, is required to confirm the role of SEE in Hall thruster characteristics at high voltage. In addition, more experimental data like the electron temperature and the ion radial velocity are needed to clarify the correlation between ion kinetic energy and power losses. Experimental values of q_p can anyway be used to refine the modeling of the near-wall sheath dynamics in a Hall thruster.

This work was carried out in the frame of the joint program CNRS/CNES/SNECMA/Universities 3161 entitled "Propulsion par plasma dans l'espace."

¹V. V. Zhurin, H. R. Kaufmann, and R. S. Robinson, *Plasma Sources Sci. Technol.* **8**, R1 (1999).

²D. M. Goebel and I. Katz, *Fundamentals of Electric Propulsion* (John Wiley & Sons, Hoboken, NJ, 2008).

³S. Mazouffre, P. Echegut, and M. Dudeck, *Plasma Sources Sci. Technol.* **16**, 13 (2007).

⁴S. Mazouffre, K. Dannenmayer, and J. Pérez-Luna, *J. Appl. Phys.* **102**, 023304 (2007).

⁵S. Barral, K. Makowski, Z. Peradzyński, N. Gascon, and M. Dudeck, *Phys. Plasmas* **10**, 4137 (2003).

⁶R. Siegel and J. R. Howell, *Thermal Radiation Heat Transfer* (Taylor & Francis, London, 2001).

⁷R. R. Hofer and A. D. Gallimore, *J. Propul. Power* **22**, 732 (2006).

⁸S. Mazouffre, V. Kulaev, and J. Pérez-Luna, *Plasma Sources Sci. Technol.* **18**, 034022 (2009).

⁹E. Ahedo and V. De Pablo, *Phys. Plasmas* **14**, 083501 (2007).

¹⁰Y. Raitses, D. Staack, M. Keidar, and N. J. Fisch, *Phys. Plasmas* **12**, 057104 (2005).